ACTA TECHNICA JAURINENSIS
Vol. XX, No. Y, pp. ZZ-ZZ, 2026
10.14513/actatechjaur.00887

Research Article

Economic and Reliability Assessment of Hybrid EV Charging Systems using Improved Coot Bird Optimisation on IEEE-33 Bus System

D. Ravi Kishore[1,*], G. Satya Narayana[1], Achanta Siva Venkat Satish[1], B. Rajesh[1], B. V. Adi Shankar Reddy[1]

[1] Department of Electrical and Electronics Engineering, Godavari Global University, NH-16, Chaitanya Knowledge City, Rajamahendravaram (Rajahmundry), Andhra Pradesh 533296, India
*Email: dravikishore@gmail.com

Submitted: 08/10/2025 *Revised: 18/11/2025* *Accepted: 19/11/2025* *Published online: 30/10/2026*

Abstract: Electric Vehicles (EVs) are crucial to the transition to sustainable transportation on a global scale due to their near-zero emissions and their ability to mitigate noise pollution. However, widespread adoption of EVs is hindered by the less accessible and high cost of Electric Vehicle Charging Stations (EVCS) for distant areas. This study addresses this issue through the development of a Hybrid Renewable Energy Sources (HRES)-based EVCS system connected to the IEEE 33 bus radial distribution network. The system incorporates a Renewable Energy System including Photovoltaic (PV) and Wind Turbine (WT), to decrease the cost of EV charging based on the renewable energy availability, and improve energy sustainability. To develop an optimized design and efficient hybrid system, this research introduces an Improved Coot Bird Optimization Algorithm (ICBOA). This improved metaheuristic algorithm quickly produces the best sizing and location for RES based on calculations intended to balance cost and reliability objectives. The reliability of the system is tested using standard reliability indices, which ensure some measure of operational stability and reliability in the energy provided. The simulation outcomes demonstrate that the proposed method has adequately reduced charging costs, improved overall reliability, and aided in achieving sustainability goals.

Keywords: Electric Vehicles; Renewable Energy Sources; IEEE-33 Bus; Electric Vehicle Charging Stations; Improved Coot Bird optimization

I. INTRODUCTION

The increasing depletion of fossil fuels, along with the severe environmental impact of their use, has accelerated the global transition to sustainable energy sources. In this scenario, EVs have been positioned as the primary method of decarbonizing the transportation sector due to their lower greenhouse gas emissions when compared to traditional vehicles, thus enhancing energy efficiency, and decrease dependence on fossil-based fuels [1]. As EVs adoption consistently rise throughout the world, the development of reliable, efficient, and cost-effective EVCS becomes crucial for the seamless and large-scale integration of EVs into existing power schemes [2]. To sustainably meet the growing energy demand of EVs, HRES such as solar PV, wind, and Battery Energy Storage Systems (BESS) are increasingly being integrated into Distribution System (DS), particularly in radial configurations. The hybrid system help to decrease environmental footprint and enhance energy availability at peak load hours, and in remote or off-grid areas. However, the non-dispatchable nature of HRES, along with the stochastic nature of EV charging behaviours, manifests in considerable planning and operational challenges [3, 4]. As a result, planning and operation of DS face several increased challenges, such as voltage spikes, increased power losses, transformer overloads, and the overall dependency on electricity generation [5].

To solve these concerns, implementing a systematic optimization-based planning method is crucial to optimally site and size Distributed Generation (DG) units, along with EV charging facilities and their load scheduling [6]. Although controlling the energy flows in a manner that minimize the overall investment cost and the power losses while maintaining the system's reliability and voltage stability [7]. Additionally, economic assessments carried out to explore options between cost-effective versus performance-based approaches

for different operational scenarios. In particular, the integration of EVCSs harms system efficiency due to high charging currents, which elevate Active Power Losses (APL) and Reactive Power Losses (RPL) [8, 9]. Furthermore, EVCS operation affects the voltage stability, potentially leading to voltage drops and fluctuations during high demand periods. In voltage stability is preserved to ensure power quality for both EV and non-EV users [10]. The reliability of Radial Distribution System (RDS) is essential for maintaining a continuous power supply, time, site location, temperature, and weather all significantly affect the energy produced by RDG sources [11, 12]. Also, the insufficient and unregulated penetration of RDG units in Distribution Networks (DNs) negatively impacts system performance, resulting in voltage instability, power losses, and decreased efficiency. Furthermore, elevated load demands from EVCSs increases the strain on network components, and increases the risk of equipment failure, and impacts the reliability of the RDS [13, 14].

Among various standard system, the IEEE-33 bus radial distribution system is a recognized standard system because of its realistic configuration, understanding of voltage sensitivity problems, and non-uniform load conditions. It allows simulating and analysing the effects of HRES integration and EVCS with constraints as a DN [15, 16]. As a result, numerous studies have focused on the ideal sizing and positioning of various types of DG units in DNs, employing advanced optimization techniques to improve system stability and dependability [17, 18].

1. Literature survey

Boonluk *et al* [19] have developed Particle Swarm Optimization (PSO) for optimizing placement and sizing of BESS within DS with integrated RES. It focusses on minimizes system cost through decreasing Voltage Deviation (VD), and power losses using IEEE 33-bus radial distribution system. However, this method relied on traditional algorithms, thus fail to evaluate the newer method of BESS, and statistically validated on larger scale systems. Khunkitti *et al* [20] have presented an optimization method using Salp Swarm Algorithm (SSA) for optimal BESS placement and sizing in DS with high levels of DG such as PV and wind. It showed improvement in system cost, voltage profile, power loss, as well as peak shaving, in IEEE 33-bus systems. However, in this system suffer to integrate with other real-time energy management systems, which limit the feasibility of the approach in constantly changing power DS. Naresh Kumar Golla *et al* [21] have implemented an Arithmetic Optimization Algorithm (AOA) to optimally place and schedule EVCS and DGs located at the IEEE 33-bus distribution system. It's improving the reduction of power losses and voltage profile by using coordinated scheduling approaches and estimating EVs and DGs. Nevertheless, by neglecting the unpredictable nature of EV charging demand and renewable generation, this method becomes less applicable inn uncertain operating environments. Md. Shadman Abid *et al* [22] have developed an Artificial Hummingbird Algorithm (AHA) to investigate optimal planning, sizing, and placement of renewable DG units in RDS based on uncertain PV and wind scenarios. The optimization to achieve a reduced power loss, improved voltage stability, decreased VD, and improved annual energy savings across IEEE 33-bus. Nonetheless, the assumptions in this study regarding planned generation and load uncertainties fail to incorporate real-time control integration and coordination of energy storage. Nandini K. Krishnamurthy *et al* [23] have introduced Modified Teaching-Learning-Based Optimization (TLBO) method using solar and wind sources to minimize charging costs for an EVCS in an IEEE 33-bus system. The application of the dynamic pricing scheme and the optimized plans for maximized use of RE using an intelligent optimization framework. However, the study does not consider the different EV user behaviours and the real charging patterns, which impact the effectiveness of this system under real operating conditions.

2. Research Gap and Novelty

Existing enhancements for the metaheuristic optimization, still experience deficiencies around narrow diversity and convergence in multi-objective problems. The proposed ICBOA specifically addresses these barriers by promoting better exploration through chaotic tent mapping, allowing for global jumps with Lévy flight, and improving local search through Cauchy mutation and OBL in the framework, while also exhibiting faster convergence and better loss and VRP improvements. This research contributes novelty in designing levelized cost and reliable hybrid EVCS utilizing ICBOA under IEEE 33-bus radial distribution network.

Key contribution of the work is

- to minimize total system cost, enhance reliability indices, and minimize technical losses for a hybrid EVCS in combination with PV and wind resources,
- proposed ICBOA is tested on IEEE-33 bus system and yields improvement in voltage stability with aggregate performance loss/reliability (APL/RPL) reduction and reliability compared to the CPSO.

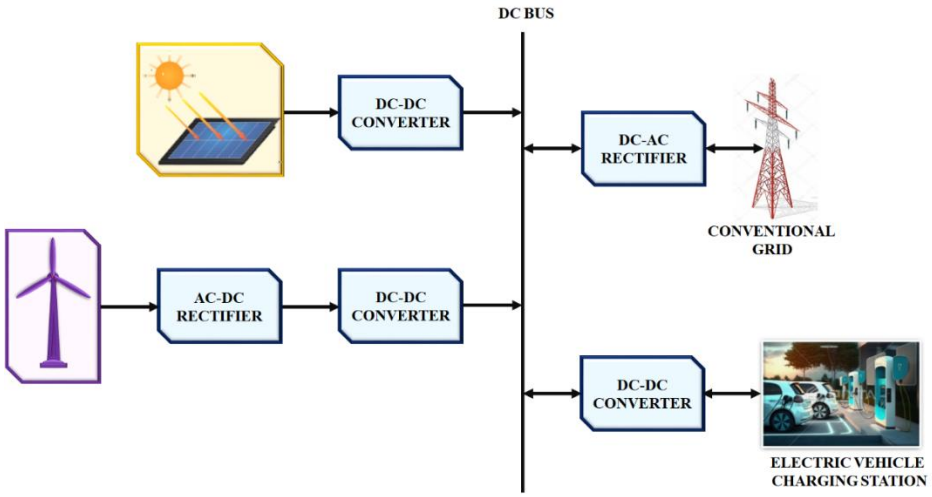


Figure 1. *Structure of RES incorporated EVCS*

II. METHODOLOGY

1. Modelling of PV system

Solar energy is vital, as it delivers clean energy to meet the global energy needs. Modelling of PV systems accurately is extremely important before implementing to understand their performance with respect to real time environmental conditions. A PV array is collected in solar model, which is linked in series-parallel configuration to attain sufficient voltage and current output. The PV modules are considered as one of the primary RES. The hourly output power of PV model, $PV_{out}(t)$ is according to subsequent relationship:

$$PV_{out}(t) = FF(t)\,.\,I_{sc}(t)\,.\,V_{oc}(t) \qquad (1)$$

Here, PV power model, $I_{sc}(t)$ denotes short-circuit current, $V_{oc}(t)$ denotes open-circuit voltage and $FF(t)$ stands fill factor at time t. These values used to control power output from PV module in response to changing environmental circumstances. The current and voltage under operational conditions are calculated as:

$$I_{SC}(t) = \frac{S}{1000}\left[I_{SC,STC} + K_i(T_c(t) - 25)\right] \qquad (2)$$

$$V_{oc}(t) = V_{oc,STC} + K_v\,(T_c\,(t) - 25) \qquad (3)$$

$$FF(t) = FF_0(t)[1 - r_{s\,(t)}] \qquad (4)$$

$$FF_0(t) = \frac{V_{oc,0}(t).\ln(V_{oc,0}(t)+0.72)}{V_{oc,0}(t)+1} \qquad (5)$$

Where, in these formulas, S stands solar irradiance at time, $I_{SC,STC}$ denotes short circuit current under standard test conditions, K_i stands current temperature co-efficient, $V_{oc,STC}$ represents open circuit voltage at STC, $FF_0(t)$ stands reference fill factor at time t. $T_c(t)$ is the module temperature, and $V_{oc,0}(t)$ is the regulated open-circuit voltage at time t. This model helps to properly estimate the output of the PV by accounting for irradiance, thermal effects, and each module characteristics.

2. Wind Turbine (WT) System

Wind energy is another growing RES, especially in rural areas where WT significantly contribute to economic growth through local electricity generation. The wind energy modeled using a WT with variable speed operation and low mechanical simplicity.

The hourly power generated by the WT is obtained from Equation,

$$P_w = \begin{cases} P_e \frac{V_t^k - V_c^k}{V_e^k - V_c^k}, & V_c \le V_t \le V_e \\ P_e, & V_e \le V_t \le V_f \\ 0\,, & V_t \le V_c \; or \; V_t \ge V_f \end{cases} \qquad (6)$$

In the above equation, P_w stands output power of turbine, P_e stands nominal power of each turbine, k is the shape parameter connecting wind speed to turbine behaviour. V_t *and* V_c denotes wind speed and cut-in speed, V_f stands cut-out speed, and V_e stands rated speed of turbine in m/s. A RES integrated EVCS is depicted in **Fig. 1**, which also indicates solar PV, WT, energy storage systems, and the utility grid are connected to deliver durable and dependable EV charging.

3. Electric Vehicle

EVs are increasingly in the attention with their eco-friendliness and growing understanding of sustainable transportation issues. The amount of power consumed by an EVCS is influenced by several important parameters: battery capacity, the type of an EV, and a critical factor is the state of charge (SoC), and the SoC depends on peculiarities of driving and charging. Each EV creates a distinguishable load profile, but each one varies depending on the several factors, resulting in

uncertainty with regards to estimating power demand. The uncertainties related to EV behaviour are modelled based on SOC, battery capacity and the types of EVs. These organizations are liable to heavily impact the accurate representation of EVs and the operation of EVCSs interconnected with hybrid renewable energy systems.

A. Battery Energy Storage System

BESS is utilized to support voltage stability, minimize power losses, and reduce grid dependency in periods of renewable energy deficits. SoC distribution is then classified into several probability scenarios based on recognized references. The dynamic change in SoC over time is determined using an expression that includes charging and discharging power, efficiencies, time intervals, and battery capacity. SoC of EVs is represented by a normal distribution that varies depending on whether the vehicle is charging or discharging and is stated as:

$$SoC(t+1) = SoC(t)\frac{P_{ch}(t))/\eta_{ch} - P_{dis}(t)/\eta_{dis}}{E_{rated}}\Delta t \quad (7)$$

Here, $P_{ch}\ and\ P_{dis}$ represents charging and discharging power, E_{rated} stands battery capacity, $\eta_{ch}\ and\ \eta_{dis}$ denotes efficacy. BESS operates within the constraints:

$$SoC_{min} \le SoC(t) \le SoC_{max} \quad (8)$$

$$0 \le P_{ch}(t), P_{dis}(t) \le P_{max} \quad (9)$$

When excess renewable generation is available, BESS stores the unused energy, however, low renewable generation or peak charging is reached the BESS is discharge to alleviate power loading on the grid. BESS operation provide essential improvements in voltage stability, reliability indices (RI), and reductions in APL/RPL in the IEEE-33 bus system. During optimization, BESS charging and discharging are part of the decision variables, allowing ICBOA to optimize operation of the BESS in combination with PV and wind to optimize overall robustness of the system.

4. Improved Coot Bird Optimization Algorithm

This section discusses the development and implementation of the ICBOA for best placement and sizing of EVCS, which are integrated with HRES, in IEEE-33 bus radial distribution network. This algorithm, an improved convergence of solution quality associated with the multi-objective optimization issue of economic cost and reliability of the system.

The basic COOT algorithm has a low diversity initial population and tends to migrate early towards local optimal values. To address the shortcomings of the COOT algorithm, this ICBOA included a chaotic tent map during initialization to increase population range, and a Lévy flight mechanism to disturb position of coots to increase the search space for the solutions. In addition, Cauchy Mutation and Opposition-Based Learning (OBL) presented near optimal region to escape local depressions and increase the accuracy of the solutions. The changes made to the basic COOT algorithm make the ICBOA a very suitable algorithm for complex multi-objective problems such as optimal placement and sizing of hybrid EVCS in DNs.

A. Initialization using Chaotic Tent map

Initial position

Coots (candidate solutions) are positioned randomly in the decision variable bounds (locations, sizes of EVCS, and capacities of RES). Chaotic maps are commonly known for randomness, and patterned behavior, and powerful tools for enriching optimization algorithms. Chaotic variables allow diversification of population during search process which enhances global search capabilities of the algorithm by mitigating premature convergence. The various chaotic maps, the tent map and logistic map are most popular. In this study, during the population initialization step, a chaotic tent map is utilized in improving coot bird optimization algorithm to diversify the method and allow robust exploration of the EVCS placement and sizing problem.

$$z_{k+1} = \begin{cases} 2z_k, & 0 < z_k < 0.5 \\ 2(1-z_k), & 0.5 \le z_k < 1 \end{cases} \quad (10)$$

$$x_j = lb_j + z_k \times \left(ub_j - lb_j\right) \quad (11)$$

Here, $lb_j\ and\ ub_j$ denotes lower and upper bounds of dimensions j. z_k stands chaotic variable. x_j denotes the j^{th} dimension of the decision variable vector.

B. Random Movement (Lévy Flight position update)

At every iteration some coots update their position in a Lévy flight to jump out of local optima. The position of a coot is changed according to:

$$Q = rand(1,d).(ub - lb) + lb \quad (12)$$

The enhanced Levy update position,

$$CootPos\ (i) = CootPos(i) + A.R_1.(Q - CootPos(i)).Levy() \quad (13)$$

C. Flocking behaviour and leader attraction

Averages the position of current and previous bird to pretend flock behaviour.

$$CootPos(i) = \frac{CootPos(i-1)+CootPos(i)}{2} \times Levy \quad (14)$$

As in the original coot algorithm, each coots update their position depend on attraction of leader. The update is defined as:

$$x_i^{t+1} = x_{leader}^t + r_1.(x_{leader}^t - x_i^t) \quad (15)$$

Where r_1 is a random coefficient [−1,1]. This allows local exploitation and it serves to accelerate convergence closer toward the optimal regions.

D. Leader based movement with Fusing Cauchy mutation ad Opposition-Based Learning

The two advanced methods, OBL and Cauchy Mutation, to be used concurrently with the ICBO algorithm, to address the premature convergence problems and improve the global search capacity of the algorithm. OBL incorporates not only a candidate solution but also its corresponding reversed solution, which allows for more efficient exploration.

$$x' = a + b - x \tag{16}$$

Here, the opposite number of x' is chosen, giving the same distance from the extremes of both bounds a *and* b. For a vector x, the reverse solution is calculated as:

$$x_i' = a_i + b_i - x_i \tag{17}$$

Calculating reverse solutions increase the chance of obtaining a better global solution, especially in the leader-following aspect of ICBOA. As stated, the leaders reverse position is calculated as:

$$X^i_{LeaderPos}\,(i) = ub + r \oplus (lb - X_{LeaderPos}(i)) \tag{18}$$

The updated best global solution is,

$$X_{GbestNew}(i+1) = X'_{LeaderPos}(i) + b_1 \oplus 2 \times R_1 \oplus \cos(2\pi R) \oplus (X'_{LeaderPos}(i) - X_{CootPos}(i)) \tag{19}$$

This hybridization enables the position both the leader and oppose of the leader, thus allowing a larger exploration.

$$f(x) = \frac{1}{\pi}\frac{T}{(x^2+T^2)} \tag{20}$$

Here, T denotes control parameter. This mutation allows longer jumps due to its heavy-tailed property which helps to improve the global search. The position of a coot bird following the Cauchy perturbation is:

$$X_{GbestNew}(i+1) = X_{CoootPos}(i) + Cauchy(0,1) * X_{CootPos(i)} \tag{21}$$

ICBOA describes in a stepwise manner the initialization of the population and the way to perform updates using advanced operators and lastly converging to attain best solution as illustrates in **Fig. 2**. The ICBOA used in defining best placement and sizing of EVCS and RES by minimizing system expenses, power losses and VD while maximizing reliability.

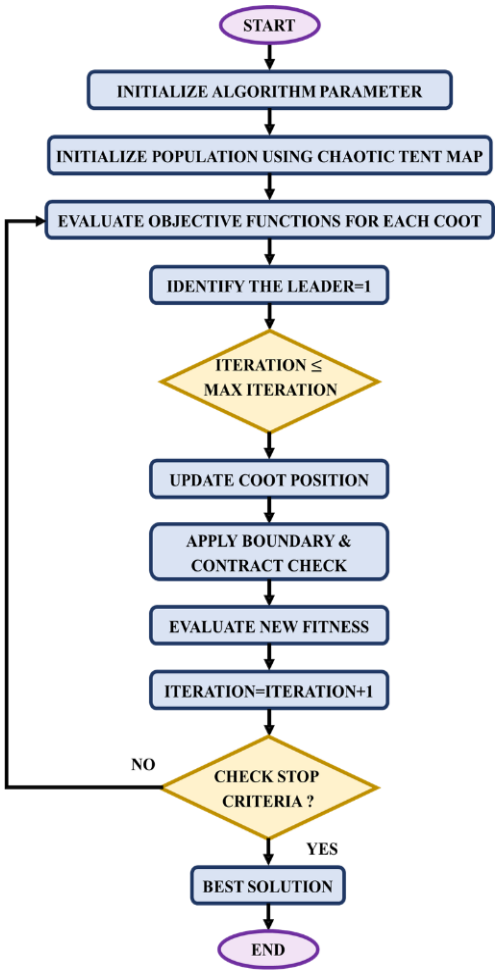


Figure 2. *Flowchart of ICBOA*

III. Problem Formulation

1. Optimization Problem Formulation for Hybrid EV charging system

The proposed work aims to optimise the IEEE 33-bus radial distribution system's EVCS and RES placement and sizing, including solar and wind. This hybrid technique improve economic performance and operational resilience of EV charging facilities depending on the time varying renewables generation.

2. Objective Function and Associated Constraints

The objective function and corresponding boundaries are as follows:

A. Economic objective function

The total system cost encapsulates the original and operational costs of the charging stations. Charge is examined for both Fast Charging Station (FCS) and Slow Charging Station (SCS).

The cost function is given by:

$$Cost = C_{installation} + C_{operation} \tag{22}$$

$$C_{installation} = \left\{\Sigma_{j=1}^{m} F_j \times f_j \times (C_{fast})\right\} + \left\{\Sigma_{j=1}^{m} S_j \times s_j \times (C_{slow})\right\} \quad (23)$$

$$C_{installation} = \left\{\left\{\Sigma_{j=1}^{m} F_j \times f_j \times (CP_{fast})\right\} + \left\{\Sigma_{j=1}^{m} S_j \times s_j \times (CP_{slow})\right\}\right\} \times P_{elec} \quad (24)$$

Here, f_j and s_j represent numbers of fast and slow charging points, accordingly, F_j and S_j stand numbers of fast and slow charging structures. The construction expenses for fast and slow charging infrastructures are denoted by C_{fast} and C_{slow}, accordingly. The power consumption of fast and slow charging structures is denoted by CP_{fast} and CP_{slow} , respectively. Price for each kWh of electricity is denoted by P_{elec}.

B. VRP (Voltage Stability, Reliability, Power Loss) Index

Each distribution unit's operational factors, including power losses, dependability, and voltage stability, are combined into a single frame. The VRP index is defined mathematically as follows.

$$VRP = w_1 \times VSI + w_2 \times R + w_3 \times P \quad (25)$$

Here, w_1, w_2 and w_3 represents weight allotted to Voltage Stability Index (VSI), Reliability (R), and Power loss (P), where

$$VSI = \frac{VSI_l}{VSI_{base}} \quad (26)$$

$$R = w_{21}\frac{SAIFI_l}{SAIFI_{base}} + w_{22}\frac{SAIDI_l}{SAIDI_{base}} + w_{23}\frac{CAIDI_l}{CAIDI_{base}} \quad (27)$$

$$P = \frac{P_{loss}^{l}}{P_{loss}^{base}} \quad (28)$$

Here, VSI_{base} and VSI_l stands before and after charging infrastructure are installed, respectively. Also, $SAIFI_{base}$ and $SAIFI_l$ stands System Average Interruption Frequency Index of the base case and after EVCS is integrated. The same notation is applied for SAIDI (System Average Interruption Duration Index) and CAIDI (Customer Average Interruption Duration Index). For weights w_1, w_2 and w_3 are allocated to SAIFI, SAIDI, and CAIDI. Additionally, P_{loss}^{l} and P_{loss}^{base} indicate the APL after EVCS deployment and base case power losses respectively.

C. Technical Constraints

The optimization problem formulation comprises of economic, reliability, and technical constraint factors to ensure the practical deployment of the RES-EVCS. The optimization problem is exposed to the following operational constraints:

- Charging Station Constraints:

$$0 < F_j \leq F_{max},\ \ 0 < f_j \leq f_{max} \quad (29)$$

$$0 < S_j \leq S_{max},\ \ 0 < s_j \leq s_{max} \quad (30)$$

Charging infrastructure constraints (Eqs. 29–30) also ensure operational safety by limiting the number and rating of charging stations to manageable values.

- Bus voltage Constraints:

$$V_j^{min} \leq V_j \leq V_j^{max} \quad (31)$$

Voltage limits (Eq. 31) ensures stable and practical operation of the IEEE-33 bus system under changing weather driven renewable input levels.

- Battery Constraints:

The battery's capacity and power are controlled to prevent overcharging or discharging, as shown in the formulas following.

$$P_{B-min} \leq P_{cha}^{t}, P_{dis}^{t} \leq P_{B-max} \quad (32)$$

$$E_{B-min} \leq E_B^t \leq E_{B-max} \quad (33)$$

Battery health state constraints (Eqs. 32–33) ensure safe battery operation both in the overcharging and discharging states and aids the overall battery health.

- Generation and Demand Balancing

$$P_{gi} - P_{di} - V_i \sum_{j=1}^{N} V_j Y_{ij} cos\left(\delta_i - \delta_j - \theta_{ij}\right) = 0 \quad (34)$$

$$Q_{gi} - Q_{di} - V_i \sum_{j=1}^{N} V_j Y_{ij} sin\left(\delta_i - \delta_j - \theta_{ij}\right) = 0 \quad (35)$$

Power balance constraints (Eqs. 34–35) ensure that the total generation meets the EVCS and network demand, for each moment of time.

- Renewable Source constraints:

$$P_{RES_{min}} \leq P_{RES_{min}} \leq P_{RES_{min}} \quad (36)$$

where P_{gi} and Q_{gi} denotes Active Power (AP) and Reactive Power (RP) generation of $i-th$ bus and P_{di} and Q_{di} denotes AP and RP demands. V_j stands voltage at the $j-th$ bus, and Y_{ij} stands distribution of bus access matrix.

IV. Results And Discussion

The proposed ICBOA-based hybrid EV charging system is utilized over the IEEE 33-bus radial distribution system network. The outcomes are showing an analysis on the voltage profile, APL, RPL, and fitness convergence for several circumstances using ICBOA and Chaotic Particle Swarm Optimization (CPSO). CPSO is employed as the benchmark as it is a well-known optimization technique for planning DS and EVCS, while ICBOA is a more enhanced algorithm that improved exploration and convergence characteristics to address the weaknesses of CPSO. This supports a clear and desired distinction when comparing the standard benchmark with the improved proposed methodology.

1. IEEE 33 bus

This section presents the results of the proposed hybrid energy system for EV charging where solar PV, and WT are combined to deliver a sustainable and reliable source of electricity with the lowest cost. The optimization carried out using the ICBO algorithm applied to the IEEE 33-bus radial distribution network. The organization of IEEE 33 bus radial distribution system as shown in **Fig. 3**, which serve as the test network for analysing the performance of Hybrid EVCS. To optimize the entire installation and ongoing operational costs, as well as the VRP index that represented voltage constancy, dependability, and power losses. The optimization objectives include placement and sizing of charging stations and renewable energy systems. The simulation conducted on a potential DN using a standard model, with all sources interfaced using the appropriate power electronic converters with each having a common DC bus voltage.

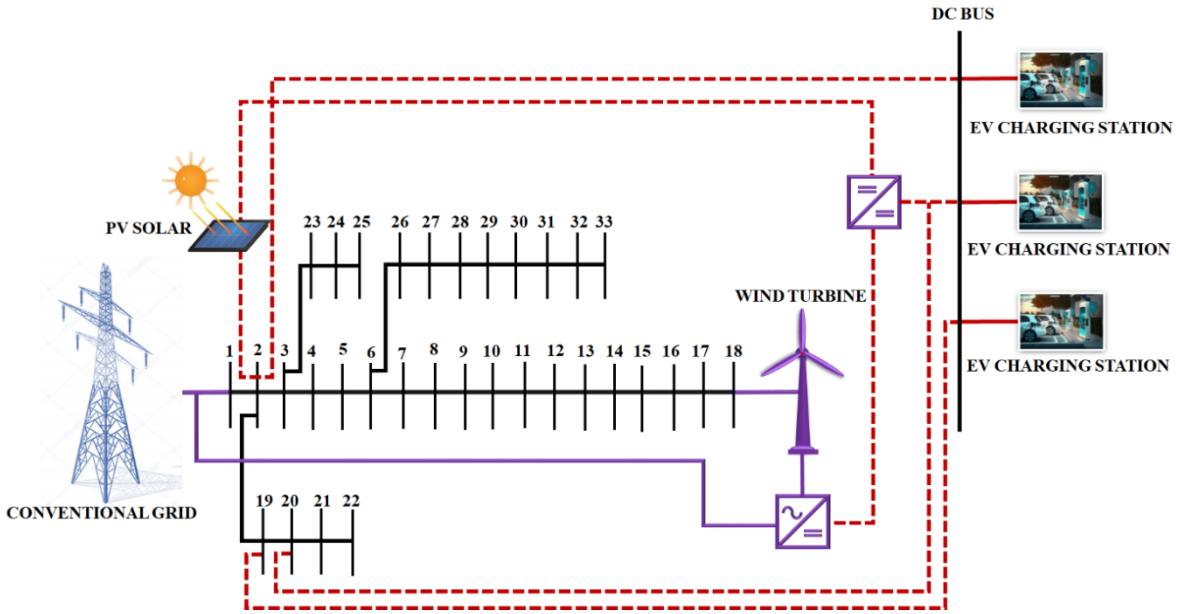
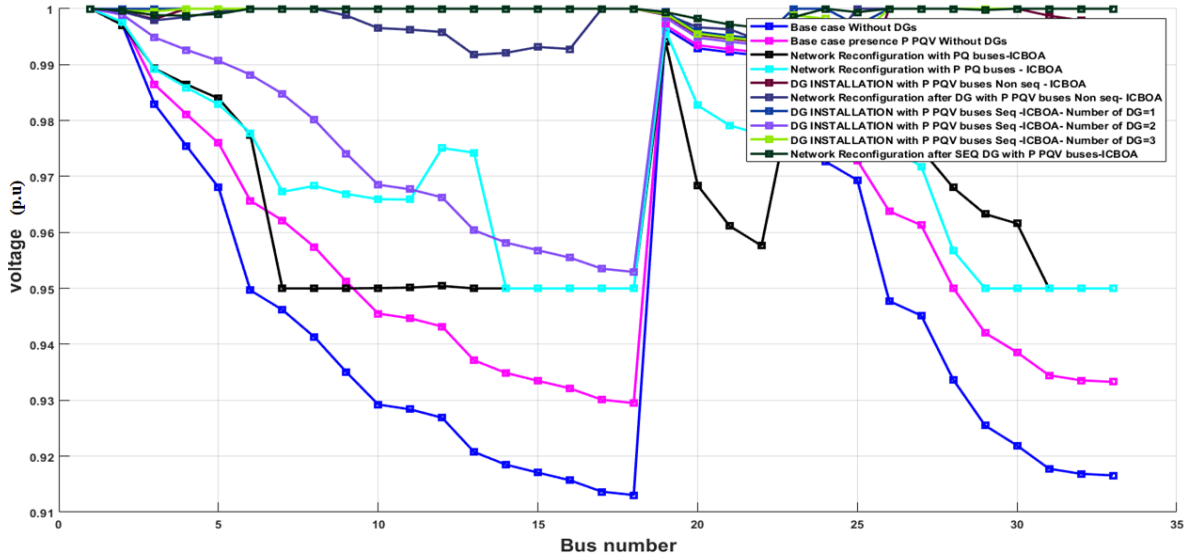


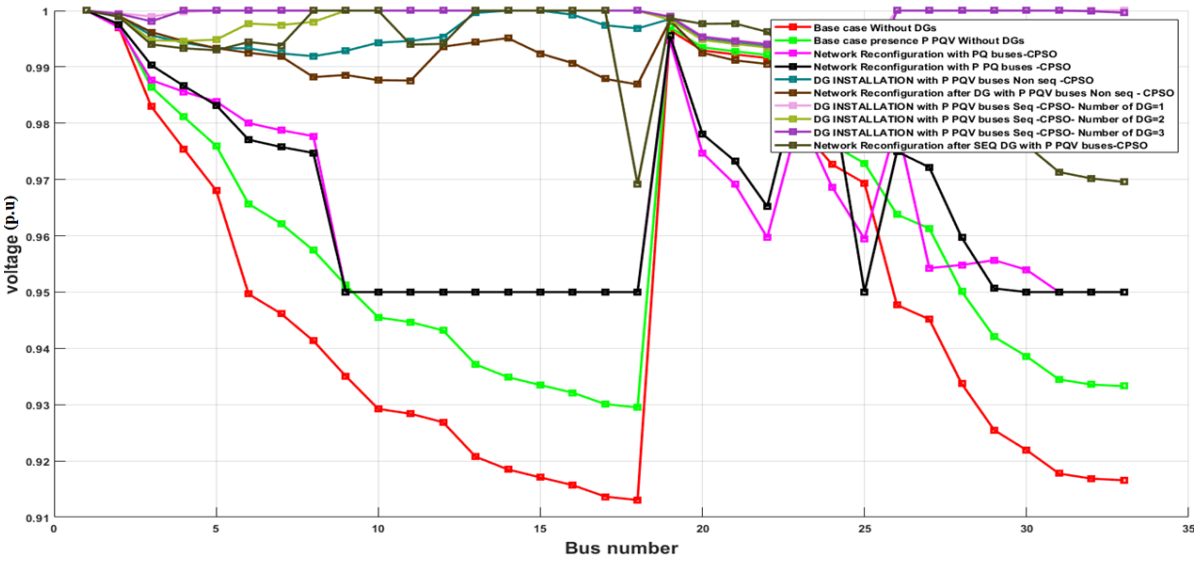
Figure 3. *Structure of IEEE 33 bus in EVCS*

The solar interfaced directly on the DC side while the wind power generated on the AC side and transformed to DC using rectification. The utility supply is to provide more resources using a bidirectional converter whenever the renewable systems are providing insufficient energy. EVCS are distributed across specific buses in the system with optimized excuses to ensure load balance and minimize voltage drops. The stations are interconnected with both directions of power transfer managed by DC-DC converters and the basis for placement is a mixture of voltage sensitivity analysis and power flow results. The system is dynamic to generation and demand diversity, with the grid supplies any power output shortfall when the RES fail to support a load. The results demonstrate that the use of ICBOA has improved convergence behavior and solution quality compared to traditional optimization methods. The system effectively balances multiple objectives, in terms of cost, and system performance, which decrease power losses, improve stability of voltage, and enhance reliability indices. In addition, placement of RESs reduce reliance on the utility grid by enhanced operating standards across a variety of loading conditions due to the integration of EVCS placement. The ICBAO is applied with a population size of 50, a maximum of 150 iterations, an inertia weight of 0.8-0.3, and a leader attraction coefficient of [-1, 1]. All simulations are run in MATLAB R2022 on a computer with an Intel i7 processor and 16 GB of RAM. Through simulations of different planning situations and configurations of the charging infrastructure, the system presented flexibility and resilience. The charging infrastructure configurations are evaluated on their ability to keep system parameters within limits of acceptable variation while still maintaining cost-effectiveness. The outcomes assist in strategic planning and process of hybrid EVCS, and deliver viable solutions for scalable, sustainable applications in future smart grid scenarios.

This result section describes the findings and interpretations in five aspects: (i) evaluation of the voltage profile, (ii) evaluation of real and reactive power loss, (iii) convergence of ICBOA and CPSO, (iv) results of DG sizing and placement, and (v) performance of the system after reconfiguration. Each result is discussed with respect to technical and economic performance.



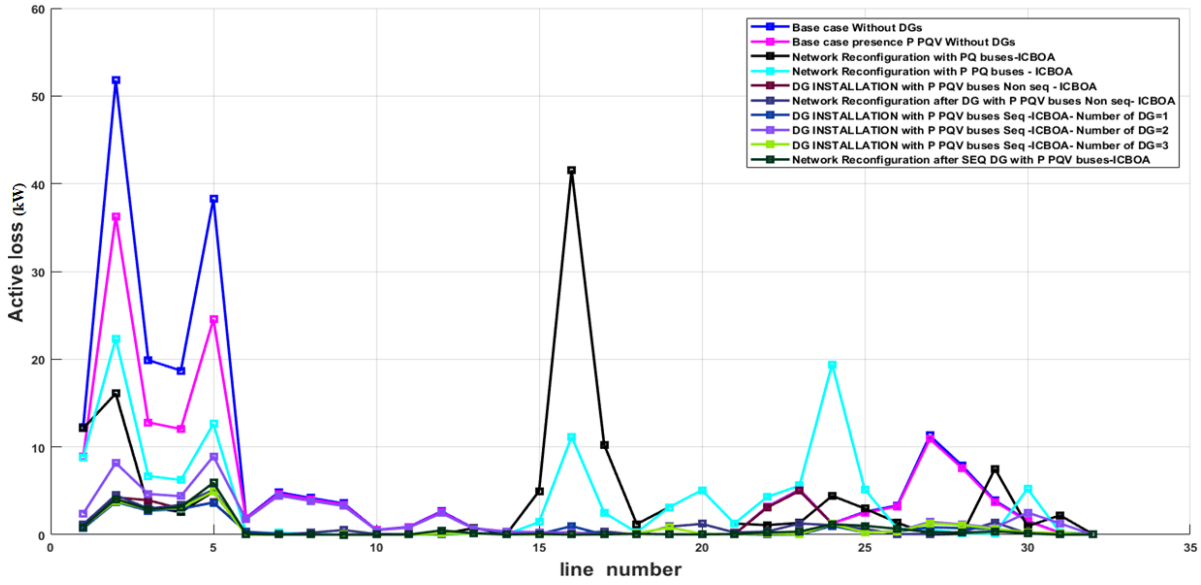
(a)



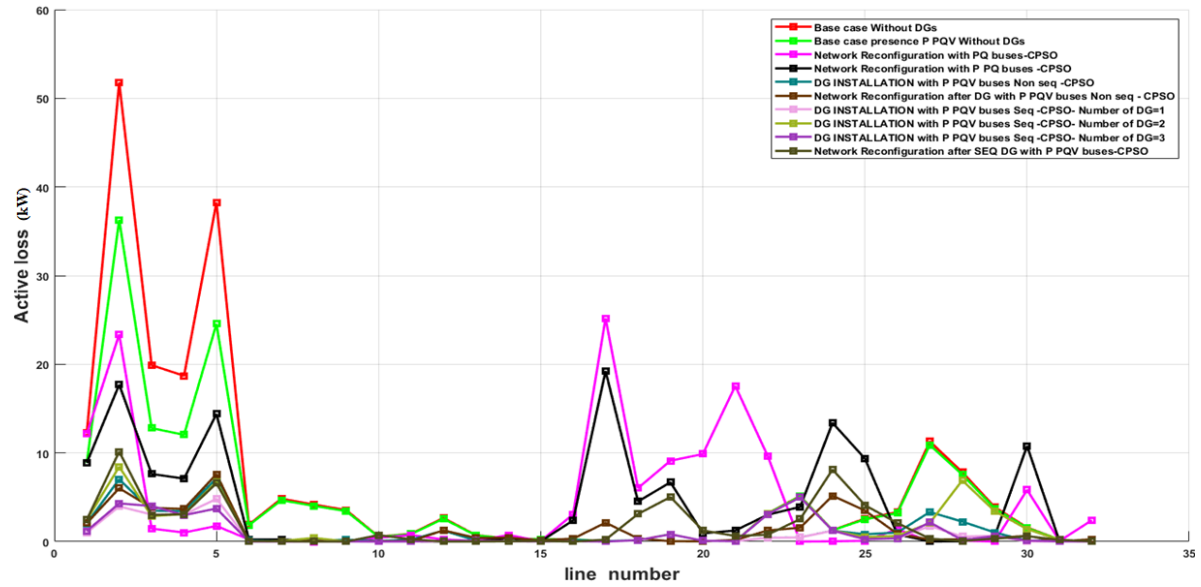
(b)

Figure 4. *Voltage profiles of the IEE 33 bus radial distributed system under various DG: (a) ICBOA and (b) CPSO*

Voltage profile throughout the IEEE 33-bus system under various situations demonstrates in **Fig. 4**. In base case without any DG combination, the system exhibits the lowest voltage level, indicating insufficient voltage stability. When P_PQV load modelling is applied without DGs, there is a slight improvement in voltage but the performance remains suboptimal. With the optimization of CPSO performed through different scenarios, such as PQ and P_PQV based reconfigurations, as well as non-sequential and sequential DG placements, the voltage improves, although it remains relatively uneven. This condition is observed to be still less uniform than the proposed application of ICBOA. Application of the ICBOA optimization, particularly in the sequential DG installations with three DGs throughout the IEEE 33-bus system, provided a clear improvement in the voltage profile throughout all buses maintaining voltage levels within the acceptable operating levels. This is evidence of the ability of IBOA to minimize voltage drop and maintain balanced voltage levels. Number of buses operating below 0.99 p.u. under various conditions clearly shows that the suggested ICBOA technique significantly reduces the number of low-voltage buses when compared to CPSO, PQ instances, and the base system, indicating its effectiveness in preserving voltage stability.



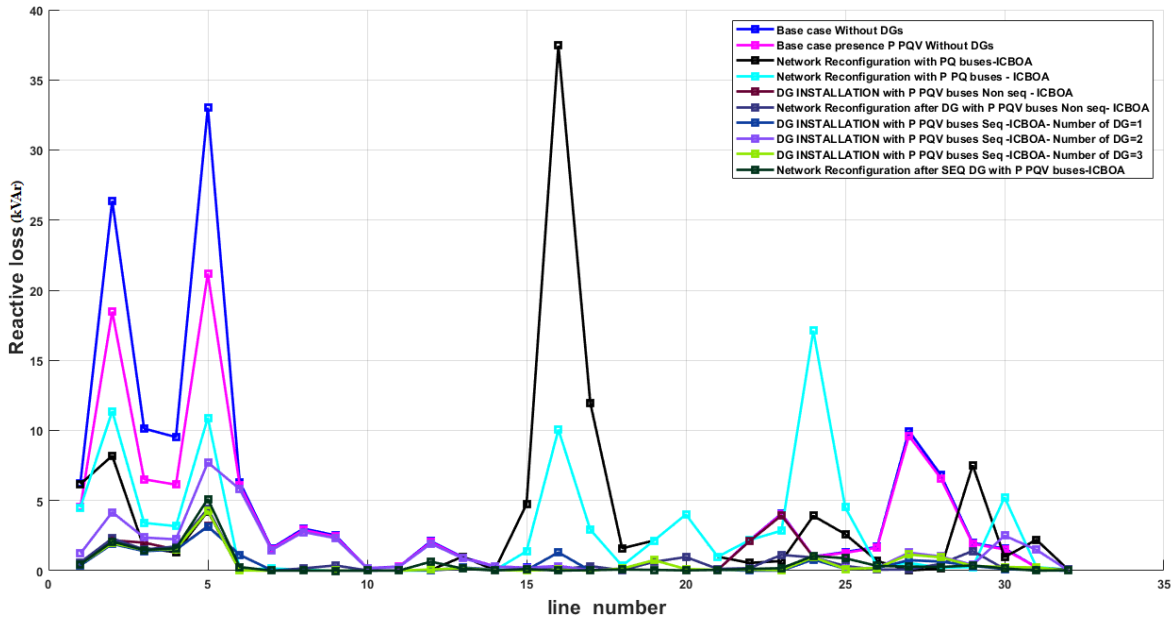
(a)



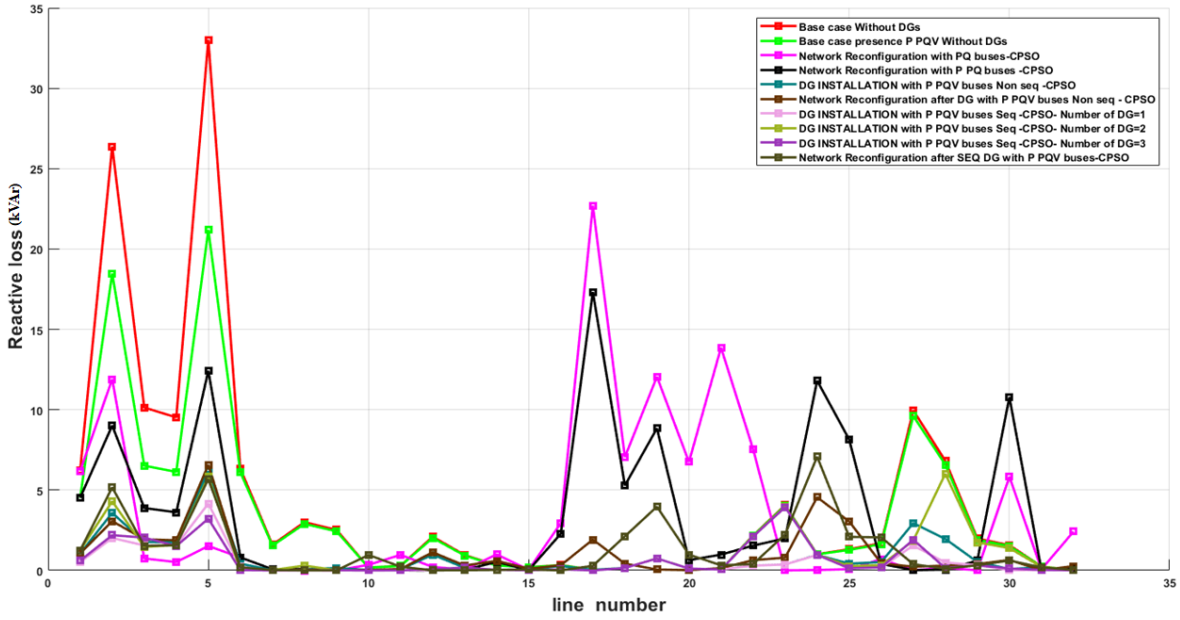
(b)

Figure 5. *APL in IEEE 33 bus radial distribution system under various DG placement: (a) ICBOA and (b) CPSO*

APL from each DG placement scenario are illustrated in **Fig. 5**. In base case without DGs, it is evident that the system experiences high APL since there is no compensation mechanism. The P_PQV load modelling scenario without DG shows slight improvement; however, the losses are still large. The scenarios with CPSO based network reconfiguration using PQ and P_PQV buses show a considerable reduction in APL. The non-sequential DG placement lead to lower APL, and some improvement as shown CPSO based sequential DG placements with PQ buses by observing the loss narrowed with each DG (1, 2, 3). The CPSO based scenarios' losses are still relatively high compared to the ICBOA instances. With ICBOA non-sequential DG installations contributed to significant reduction in APL, and the effects are magnified with subsequent sequential installations. Among the four activated scenarios, the ICBOA sequential DG installation with three DGs had the highest order of optimization by limiting APL in the system.



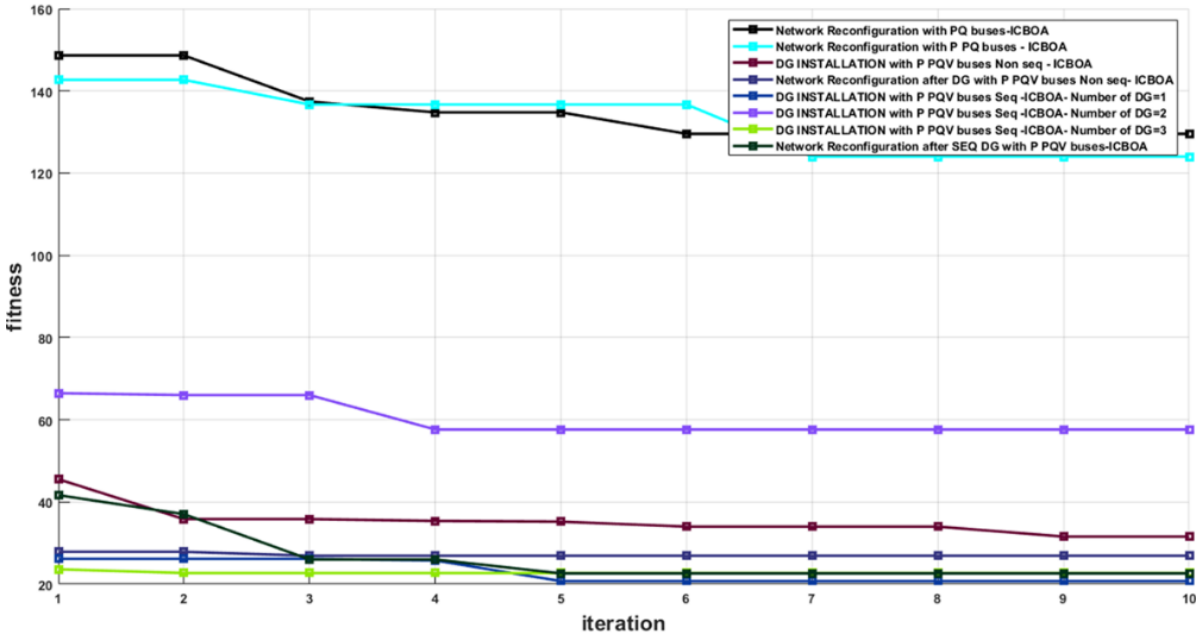
(a)



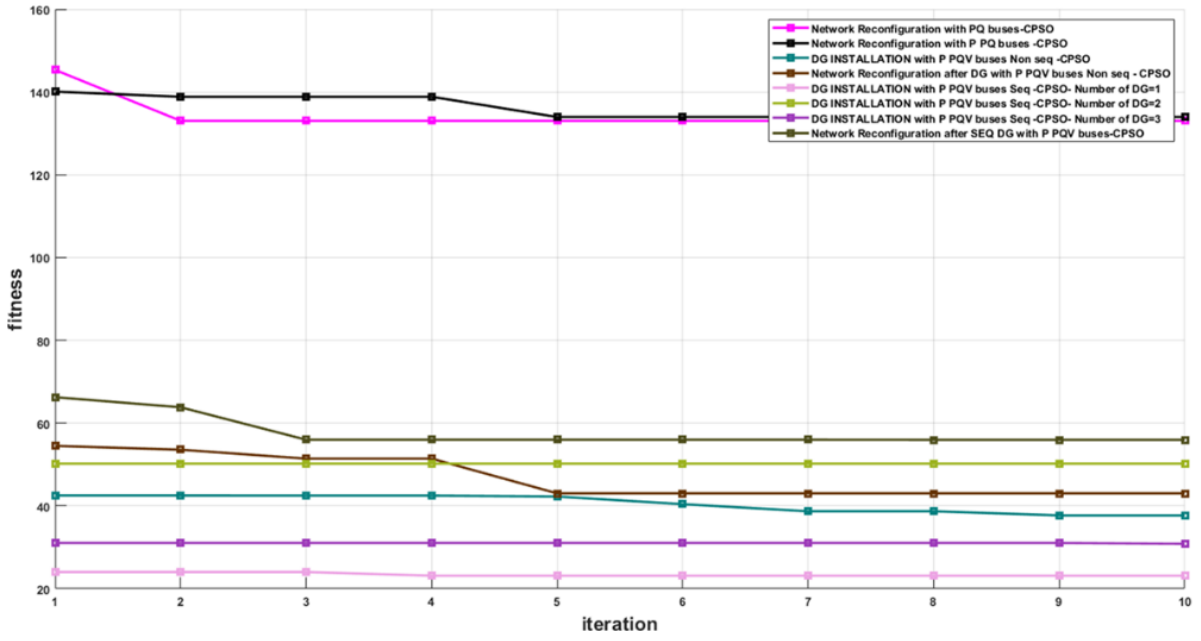
(b)

Figure 6. *RPL under various optimization and DG integration scenarios: (a) ICBOA and (b) CPSO*

RPL provided in **Fig. 6** shows under different conditions. The base case is without DGs, which showed the largest RPL, generally due to a radial network and without distributed generation in the network. P_PQV modelling without DG also shows minimal loss reduction. The configuration using CPSO with PQ and P_PQV bus reconfiguration shows a modest loss reduction. Non-sequential and sequential allocation of DG shows further improvements using CPSO, and with additional DG the reduce losses. In all cases ICBOA based configuration outperformed the other methods for loss reduction. The non-sequential DG placement using ICBOA provided improvements to RPL, and sequential DG placement provided further improvements. The greatest improvement achieved when three DGs were placed sequentially using ICBOA, resulting in the lowest RPL across all the cases. Therefore, findings indicate that ICBOA is able to identify the optimally located and sized DG units, by providing the least amount of RPL across the entire DS.



(a)



(b)

Figure 7. *Convergence behaviour of the fitness value over various DG: (a) ICBOA and (b) CPSO*

The evolution of convergence in fitness values for all approaches is shown in **Fig. 7**. The CPSO method the slowest and most unstable across all cases and generally had to evolve for more iterations to obtain a near-optimal solution. The non-sequential and sequential DG solutions for most approaches based on increased or substantial fitness, but the convergence still slow and inconsistent. The ICBOA method performed the best and provided consistent and speedy convergence results. Whether using a non-sequential or sequential method, the fitness improved in a short amount of iterations. The best convergence performance observed in the case of three sequential DG units with the ICBOA approach.

The proposed ICBOA has better performance because it combines a number of enhancement mechanisms. Search diversity is enhanced by initiating the search with Chaotic Tent, which helps avoid clustering reactions around the early solutions. Lévy flight broadens the global search space, so that the ICBOA is able to escape local minima faster than CPSO. Furthermore, the combination of Cauchy mutation + opposition-based learning, offers great exploitation capabilities around optimal areas, while

assuring population diversity. These joint mechanisms allow the ICBOA to achieve faster convergence, greater stability, and more accurate identification of DG sizes/locations for EVCS.

Table 1. *Baseline results without DGs*

Parameters	***Real power loss*** (kW)	***Reactive power loss*** $(kVAr)$	***Total real power load*** (kW)	***Total reactive power load***$(kVAr)$	***Branches open***
Base case without DGs	203.1	134.93	3716	2302	8-21,9-15,12-22,18-33,25-29

This table (**Table 1**) presents the baseline performance of IEEE 33-bus distribution system without DG. RDS shows considerable real power loss $(203.1\ kW)$ and RPL $(134.93\ kVAr)$, which attributed to the radial configuration and the absence of generation close to the load. The total load on the system is $3716\ kW$ (real) and $2302\ kVAr$ (reactive), with specific branches (8-21), (9-15), (12-22), (18-33), and (25-29), which kept to maintain the system radial.

Table 2. *Network Reconfiguration result with PQ and P_PQV buses*

Optimization Methods	***PQ buses***		***P_PQV buses***	
	CPSO	***ICBO***	***CPSO***	***ICBO***
Real power loss (kW)	133.0306	133.3609	133.949	124.4487
Reactive power loss $(kVAr)$	106.6421	95.7787	105.9572	91.4866
Real power loss reduction	34.3633	34.2003	13.2697	19.421
Branches open	9-10,26-27,8-9,30-31	9-10,7-8,12-13	31-32,8-9,14-15,24-25	11-12,8-9,17-18
Branches closed	8-21	18-33,25-29	8-21	8-21,25-29

Table 2 displays the results comparing the CPSO results and ICBOA for PQ and P_PQV bus configurations. In PQ bus configurations, ICBOA achieves a real power loss of $133.36\ kW$, and a RPL of $95.78\ kVAr$; compared to CPSOs results of $133.03\ kW$ for real power loss, and $106.64 kVAr$ for RPL. Although real losses are close, ICBOA works better for RPL while also using a better switching strategy. In the P_PQV bus cases fits has clear advantages over the CPSO results of $133.95 kW$ real power loss, and $105.95\ kVAr$. ICBOA shows clear superiority with a real power loss of $124.45\ kW$, and a RPL of $91.48\ kVAr$. The results also confirm ICBOAs loses found the maximum reduction in real power loss $(19.42\ kW)$ compared to CPSO $(13.27 kW)$ confirming the ICBOA's effective capabilities found under realistic conditions.

Table 3. *DG Installation with P_PQV buses*

Optimization Methods	***CPSO***	***ICBO***
Real power loss (kW)	37.7132	23.829
Reactive power loss $(kVAr)$	26.0349	17.4846
Real power loss reduction	75.5811	84.571
Branches open	8-21,9-15,12-22,18-33,25-29	8-21,9-15,12-22,18-33,25-29
DG Size	531 579 779	961 853 958
DG location	32 24 14	24 17 33

Table 3 compares DG installation to optimize for P_PQV load modeling with CPSO and ICBOA. ICBOA has $23.829\ kW$ in real power loss to $37.713\ kW$ with CPSO, with ICBOA also having a percentage reduction is greater. The optimal DG sizes and locations differ between the two methods, with ICBOA placing larger units at buses 24, 17, and 33, compared to buses 32, 24, and 14 with CPSO. This shows that ICBOA more effectively identifies high-impact locations and sizes for DG units to maximize system performance.

Table 4 displays outcome of reconfiguration network after DG connection, with P_PQV bus modelling, using CPSO and proposed ICBOA. The outcome achieved by ICBOA a real power loss of $37.61\ kW$ compared to $43.04\ kW$ (CPSO) and RPL are $28.53\ kVAr$ (ICBOA) compared to $31.29\ kVAr$ (CPSO). The real power loss reduction realized $75.65\ kW$ compared to CPSO which is $72.13\ kW$. The branch switching combination realized within ICBOA clearly a more desirable combination by opening branches 7-8, 12-13, 30-31, 21-22 and

closing 25-29. The results confirm that ICBOA is the most effective method for minimizing losses and optimizing the DN once the DG has been implanted.

Table 4. *Reconfiguration network topology after DG with P_PQV buses*

Optimization Methods	***CPSO***	***ICBO***
Real power loss (kW)	43.0372	37.6104
Reactive power loss ($kVAr$)	31.2935	28.5306
Real power loss reduction	72.1339	75.6477
Branches open	32-33,23-24,7-8,11-12	7-8,12-13,30-31,21-22
Branches closed	12-22	25-29

Table 5. *DG Installation with P_PQV buses (sequential)*

Optimization Methods	***DG=1***		***DG=2***		***DG=3***	
	CPSO	***ICBO***	***CPSO***	***ICBO***	***CPSO***	***ICBO***
Real power loss (kW)	23.1477	19.5283	50.2312	52.0183	30.8497	26.7415
Reactive power loss ($kVAr$)	15.769	14.0373	35.1609	36.8974	20.9812	18.378
Real power loss reduction	85.0121	87.3557	67.4759	66.3188	80.0252	82.6852
Branches open	8-21,9-15,12-22,18-33,25-29		8-21,9-15,12-22,18-33,25-29,		8-21,9-15,12-22,18-33,25-29,'	
DG Size	732	1000	732 989	1000 1000	732 989 744	1000 1000 981
DG Location	28	26	28 13	26 31	28 13 28	26 31 13

Table 5 displays the performances of CPSO and ICBOA for each sequential DG installation (DG=1, DG=2, DG=3) in the P_PQV bus configuration. With DG=1 connected, ICBOA the least amount of real loss and RPL ($19.53\ kW, 14.04\ kVAr$) compared to CPSO ($23.15\ kW, 15.77\ kVAr$) and has the largest power loss reduction amount ($87.36\ kW$). For DG=2, CPSO has $50.23\ kW$ real loss and $35.16\ kVAr$ RPL. ICBOA has slightly greater real loss of (52.02 kW) but performed better by continually producing greater network stability with effective sizing and siting of local DG resources. For DG=3, ICBOA performed better than CPSO, as it exhibited the lowest real power loss ($26.74\ kW$) and RPL ($18.38\ kVAr$) with a total power loss reduction of $82.69\ kW$ (compared to 80.03 kW from CPSO). In addition, ICBOA found more effective DG sizes and locations (up to a maximum of $1000\ kW$ at buses 26, 31, and 13) ensuring effective load balancing and loss minimization in the DN.

Table 6. *Network Reconfiguration after SEQ_DG with P_PQV buses*

Optimization Methods	***CPSO***	***ICBO***
Real power loss (kW)	55.9586	20.6473
Reactive power loss ($kVAr$)	39.9653	13.9208
Real power loss reduction	63.7675	86.6311
Branches open	17-18,10-11,12-13,7-8	24-25,11-12,8-9,19-20
Branches closed	25-29	8-21

Table 6 displays the network reconfiguration results after the sequential DG installation using CPSO and ICBOA under P_PQV bus model. The results show that ICBOA significantly outperformed CPSO, with a lower real power loss of 20.65 kW compared to CPSO producing 55.96 kW. In a similar fashion, ICBOA provides a lower RPL of 13.92 $kVAr$ while CPSO achieved $39.97\ kVAr$. The amount of real power loss reduction with ICBOA $86.63\ kW$ compared to CPSO's $63.77\ kW$. ICBOA also opened different branch pairs when identifying the activated branches (24-25, 11-12, 8-9, 19-20) and closed branch 8-21 suggesting that the opening and closing configuration with ICBOA is more efficient than that of CPSO. Based on the results, ICBOA shows better performance with reducing losses and improving DNs performance during sequential DG planning.

Table 7. *Enhancement of ICBOA compared to CPSO*

Metric	*CPSO*	*ICBOA*	*% Improvements*
Real Power Loss	37.7	23.8	36.9%
Reactive Power Loss	26	17.4	33%
Convergence Iterations	68	34	50% faster

ICBOA consistently outperforms CPSO across all performance criteria. Table 7 summarises the percentage gains, highlighting the ICBOA benefit in convergence speed, and loss minimisation. The computational complexity of the proposed ICBAO is,

$$O\,(N \times D \times T),$$

Where N is the population size, D is the number of decision variables, and T is the number of iterations. In practical simulations, ICBAO averaged 1.42 seconds per run compared to 2.87 seconds for CPSO, indicating a convergence 50% faster due to better exploration–exploitation balance.

V. Conclusion

In this study presented, a hybrid EVCS integrated with RES has been effectively optimized using the ICBOA for the IEEE 33-bus radial distribution system. This novel approach has identified optimal siting and sizing requirements for renewable energy units and EVCS. The proposed optimization approach able to significantly reduce APL and RPL within the network. The voltage profile across the network improved significantly, and the voltage stability improved even under dynamic load variations. In addition, the reliability of the system increased with the inclusion of reliability indices. The reliability indices proven to the improvement in reliability for the proposed optimization procedures. The ICBOA algorithm assured faster convergence and better solution quality over the CPSO algorithm which serves as the benchmark in the study. In addition, the inclusion of uncertainty modelling regarding EV battery SoC, battery capacity, and vehicle type in the optimization process allow for a better representation of the charging behavior that is representative of reality. The proposed method is efficient in improving economic performance, reliability, and operational resilience to improve hybrid EV charging infrastructures in the future. Also, the proposed method is more than capable of addressing future smart and sustainable DS. The proposed ICBOA-based hybrid EVCS framework has to address numerous real world considerations associated with renewable intermittency, grid constraints, limited investment capabilities, and reliable communication and controls are necessary for real world implementations.

Author Contributions

D. Ravi Kishore: Conceptualization, Methodology, Data Curation, Writing – Original Draft.

G. Satya Narayana: Methodology, Project Administration, Validation, Investigation, Writing – Review & Editing

Achanta Siva Venkat Satish: Project Administration, Supervision, Visualization, Writing – Review & Editing

B. Rajesh: Supervision, Resources, Visualization, Validation, Writing – Review & Editing

B.V. Adi Shankar Reddy: Investigation, Resources, Supervision, Validation, Writing – Review & Editing

Disclosure Statement

The authors declare that they have no known competing financial interests or personal relationships that could have appeared to influence the work reported in this paper.

ORCID

D. Ravi Kishore https://orcid.org/0000-0001-5065-5177

G. Satya Narayana: https://orcid.org/0009-0003-1412-7205

Achanta Siva Venkat Satish: https://orcid.org/0009-0006-3823-4605

B. Rajesh: https://orcid.org/0009-0003-5970-343X

B. V. Adi Shankar Reddy: https://orcid.org/0009-0005-3848-2468

Reference

[1] K. Vaishali, D. R. Prabha, The reliability and economic evaluation approach for various configurations of EV charging stations, IEEE Access 12 (2024) pp. 26267-26280. https://doi.org/10.1109/ACCESS.2024.3367133

[2] N. Rehman, M. U. D. Mufti, N. Gupta, Metaheuristic method for a wind-integrated

distribution network to support voltage stabilisation employing electric vehicle loads, Applied Sciences 13 (4) (2023) pp. 2254. https://www.mdpi.com/2076-3417/13/4/2254#

[3] S. Vendoti, T. A. Kiran, T. T. Thangam, R. S. Nagini, K. S. Kavin, B. A. Rahiman, A PV Fed Grid Connected SEPIC-ZETA Converter Along with High Frequency Isolation Fly Back Converter for Multiport EV Applications, In 2024 2nd International Conference on Computer, Communication and Control (IC4), (2024) pp. 1-7. https://doi.org/10.1109/IC457434.2024.10486450

[4] R. Chakraborty, P. Das, D. Das, P. Das, S. Gope, A. R. Bhowmik, Reliability-Driven Strategic Allocation of Renewable Integrated EV Charging Infrastructure in Radial Distribution System, In 2024 IEEE Silchar Subsection Conference (SILCON 2024), (2024) pp. 1-6. https://doi.org/10.1109/SILCON63976.2024.10910362

[5] R. Sripriya, C. Kumar, F. J. Xavier, J. S. Kumar, P. Kotsampopoulos, H. H. Fayek, Reliability improvement of a hybrid electric vehicle integrated distribution system, Energies 16 (10) (2023) pp. 3984. https://doi.org/10.3390/en16103984

[6] A. M. Faizal, E. Maheswari, P. Raviteja, K. S. Kavin, S. Chithra, A. R. Gayathri, Improved Boost Converter for Solar System in Grid Connected EV Charging Station, In 2024 International Conference on Recent Advances in Electrical, Electronics, Ubiquitous Communication, and Computational Intelligence (RAEEUCCI), (2024) pp. 1-6. https://doi.org/10.1109/RAEEUCCI61380.2024.10547918

[7] K. K. Nandini, N. S. Jayalakshmi, V. K. Jadoun, Optimization of distribution network operating parameters in grid tied microgrid with electric vehicle charging station placement and sizing in the presence of uncertainties, International Journal of Green Energy 22 (8) (2025) pp. 1552-1569. https://doi.org/10.1080/15435075.2023.2281334

[8] M. Z. Islam, M. L. Othman, N. I. Abdul Wahab, V. Veerasamy, S. R. Opu, A. Inbamani, V. Annamalai, Marine predators algorithm for solving single-objective optimal power flow, PLoS One 16 (8) (2021) pp. e0256050. https://doi.org/10.1371/journal.pone.0256050

[9] S. K. Szürke, I. Lőrincz, Opportunities for Pulse-Based Diagnostics in Electric and Hybrid Vehicle Batteries, In 2025 19th Conference on Electrical Machines, Drives and Power Systems (ELMA) (2025) pp. 1-4. IEEE. https://doi.org/10.1109/ELMA65795.2025.11083486

[10] B. V. Kumar, A. Farhan, Optimal Integration of EV Charging Stations and Capacitors for Net Present Value Maximization in Distribution Network, IEEE Latin America Transactions 23 (3) (2025) pp. 239-250. https://doi.org/10.1109/TLA.2025.10879176

[11] V. Veerasamy, N.I. Abdul Wahab, A. Vinayagam, M.L. Othman, R. Ramachandran, A. Inbamani, H. Hizam, A novel discrete wavelet transforms based graphical language classifier for identification of high impedance fault in distribution power system, International Transactions on Electrical Energy Systems 30 (6) (2020) pp. e12378. https://doi.org/10.1002/2050-7038.12378

[12] W. K. M. Al-Zaidi, A. Inan, Optimal placement of battery swapping stations for power quality improvement: A novel multi techno-economic objective function approach, Energies 17 (1) (2023) pp. 110. https://doi.org/10.3390/en17010110

[13] I. Abinaya, RR Rubia Gandhi, H. Vidhya, M. Karthik, R. Thangaraj, Demand Side Management for Motoring and Lighting Loads, International Journal of Research in Engineering, Science and Management.

[14] F. Alanazi, M. Bilal, A. Armghan, M. R. Hussan, A metaheuristic approach based feasibility assessment and design of solar, wind, and grid powered charging of electric vehicles, IEEE Access 12 (2024) pp. 82599-82621. https://doi.org/10.1109/ACCESS.2024.3411291

[15] S. B. Thanikanti, T. Yuvaraj, R. Hemalatha, B. Aljafari, N.I. Nwulu, Optimizing radial distribution system with distributed generation and EV charging: a spotted hyena approach, IEEE Access 12 (2024). https://doi.org/10.1109/ACCESS.2024.3438456

[16] S. Kocsis Szürke, R. Pál, G. Saly, Analysis of the Correlation Between Electric Bus Charging Strategies and Carbon Emissions from Electricity Production. World Electric Vehicle Journal 16 (4) (2025) pp. 240. https://doi.org/10.3390/wevj16040240

[17] J. A. J. Shirley, R. P. Pooja, M. J. B. Reddy, Metaheuristic Algorithm Based Energy Management System for Electric Vehicle Charging Station, IEEE Access 12 (2024). https://doi.org/10.1109/ACCESS.2024.3446032

[18] S. K. Szürke, G. Saly, I. Lakatos, Analyzing Energy Efficiency and Battery Supervision in Electric Bus Integration for Improved Urban Transport Sustainability, Sustainability 16 (18) (2024) pp. 8182.

https://doi.org/10.3390/su16188182

[19] P. Boonluk, A. Siritaratiwat, P. Fuangfoo, S. Khunkitti, Optimal siting and sizing of battery energy storage systems for distribution network of distribution system operators, Batteries 6 (4) (2020) pp. 56. https://www.mdpi.com/2313-0105/6/4/56#

[20] S. Khunkitti, P. Boonluk, A. Siritaratiwat, Optimal location and sizing of BESS for performance improvement of distribution systems with high DG penetration, International Transactions on Electrical Energy Systems 2022 (1) (2022) pp. 6361243. https://doi.org/10.1155/2022/6361243

[21] N. K. Golla, S. K. Sudabattula, V. Suresh, Optimal placement of charging station and distributed generator along with scheduling in distribution system using arithmetic optimization algorithm, Int. J. Renew. Energy Res. IJRER 12 (2) 2022.

[22] M. S. Abid, H. J. Apon, K. A. Morshed, A. Ahmed, Optimal planning of multiple renewable energy-integrated distribution system with uncertainties using artificial hummingbird algorithm, IEEE Access 10 (2022) pp. 40716-40730. https://doi.org/10.1109/ACCESS.2022.3167395

[23] N. K. Krishnamurthy, J. N. Sabhahit, V. K. Jadoun, D. N. Gaonkar, A. Shrivastava, V. S. Rao, G. Kudva, Optimal placement and sizing of electric vehicle charging infrastructure in a grid-tied DC microgrid using modified TLBO method, Energies 16 (4) (2023) pp. 1781. https://doi.org/10.3390/en1604178

This article is an open access article distributed under the terms and conditions of the Creative Commons Attribution NonCommercial (*CC BY-NC 4.0*) license.